Title: RESULTS FROM RECENT ROTATING MAGNETIC FIELD EXPERIMENTS ON TCS

Author(s): H.Y. Guo (UW), R.D. Brooks (UW), W.A. Crawford (UW) A. L. Hoffman (UW), P. Melnik (UW), R.D. Milroy (UW), M. Peter (UW) Z.A. Pietrzyk (UW), J.T. Slough, (UW) G. R. Votroubek (UW), S.V. Tobin (P-24)

Submitted to: US-Japan
Workshop on Physics of Innovative High Beta Concepts
February, 26, 2001-March 2, 2001

Results from Recent Rotating Magnetic Field Experiments on TCS

H.Y. Guo, R.D. Brooks, E.A. Crawford, A.L. Hoffman, P. Melnik, R.D. Milroy, M. Peter, Z.A. Pietrzyk, J.T. Slough, S.J. Tobin*, G.R. Votroubek
Redmond Plasma Physics Laboratory
University of Washington
**Los Alamos National Laboratory, MS-E526, Los Alamos*

1. Introduction

The Field Reversed Configuration (FRC) is attractive for the design of a magnetic fusion reactor because of its intrinsically high plasma beta, natural divertor, and engineering simplicity. The lifetime of FRCs produced by the conventional field reversed theta pinch (FRTP) method is restricted to only hundreds of microseconds due to resistive flux losses. Rotating Magnetic Field (RMF) offers a promising tool for toroidal current drive in FRCs and maintaining the configurations in steady state.

Steady state RMF current drive is achieved as the force exerted on the electrons by the RMF is balanced by the resistive friction force, which can be expressed in terms of ratio of RMF drive parameter γ to the penetration parameter λ [1]:

$$\frac{\gamma}{\lambda} = \frac{0.07 B_\omega}{n_m D_\perp^{1/2} (\omega r_s^2)^{1/2}} = \frac{1}{\sqrt{2}} \qquad (1)$$

where B_ω is strength of rotating field (in G), n_m central density (10^{19} m^{-3}), $D_\perp$ perpendicular resistivity (m^2/s), ω frequency of RMF (MHz), and r_s separatrix radius (m). The maximum sustainable magnetic field is determined by the toroidal current that can be produced by the RMF and is given by:

$$B_e = \frac{500 \langle \beta \rangle \zeta (\omega r_s^2)^{1/2} B_\omega}{D_\perp^{1/2}} \qquad (2)$$

where ζ is defined as the ratio of the current required to reverse the external magnetic fields to the maximum synchronous current that can be driven by the RMF: $\zeta = \frac{B_e}{5000 \langle n \rangle (\omega r_s^2)}$, with B_e in G and averaged plasma density $\langle n \rangle$ in 10^{19} m^{-3}.

2. Steady-State Current Drive in TCS

RMF has been applied to the new Translation, Confinement and Sustainment (TCS) device, producing, for the first time, nearly steady state FRCs with configuration lifetime over 1 ms (the entire duration of RMF).

To demonstrate this, Fig. 1 shows the time traces for pulse 1932 with RMF operated at $\omega = 1$ MHz. RMF is applied to a preinoized gas in a uniform bias field of 60 G, producing fully reversed field configuration with an external field reaching ~ 150 G, which is over 4 times the applied RMF field. The evolution of the FRC is quantitatively reproduced by

an analytical model with $D_\perp$ = 115 m^2/s [1].

To improve RMF current drive efficiency, we have carried out experiments with RMF frequency reduced from initial 1 MHz to 0.5 MHz.

Fig. 2 compares two discharges with similar RMF heating power, but with different frequencies. As can be seen, at reduced ω, FRC peak density (n_m) increases, as predicted by the steady state RMF current drive requirement: $n_m \propto B_\omega D_\perp^{-1/2} (\omega r_s^2)^{-1/2}$. The external magnetic field (B_e) is also higher for the reduced ω case despite lower ω, suggesting ζ is higher, thus better RMF current drive efficiency.

In addition, reducing RMF frequency reduces the impedance (ωL) of the antenna tank circuit, resulting in a higher antenna current, thus allowing for higher RMF field for a given pulsar voltage. This, in turn, leads to higher B_e and n_e, as expected [see Eqs. (1) and (2)].

Fig. 3 plots B_e as a function of B_ω achieved during the steady state phase of the discharges with RMF operated at both 1 MHz and 0.5MHz. In addition, An STX result is also shown for comparison.

As can be seen, B_e shows a nearly linear dependence on the RMF field, independent of ω. This is because RMF current drive efficiency (ζ) is improved at reduced ω, thus offsetting the effect of reduced ω in Eq. (2), as discussed earlier (STX operated at the same ωr_s^2 as TCS, 2.2MHz and 20cm, but at relatively

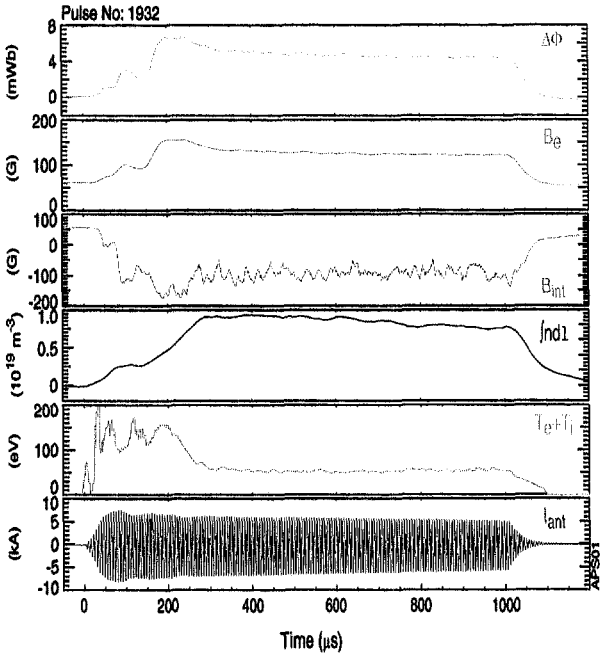

Figure 1. Time evolution of the FRC produced and maintained in steady state by the RMF.

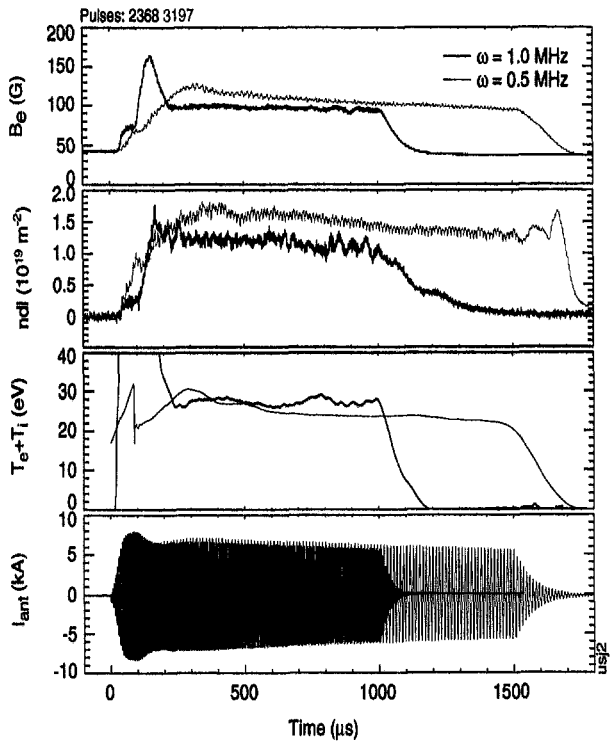

Figure 2. Comparison of discharges with RMF operated at ω = 1 and 0.5MHz, respectively.

lower density, thus higher ζ). To further improve performance (at a given RMF field), it is essential to reduce the anomalous diffusivity ($D_\perp$) and increase the plasma temperature (increasing temperature results in a lower density and the ability to operate at increased ω with the same ζ).

Figure 4(a) shows the diffusivity derived from $\gamma/\lambda=1/\sqrt{2}$ for the steady state discharges with ω = 1.0 MHz and 0.5 MHz. The prediction from conventional high density (LSX) FRC scaling: $D_\perp = 10\ x_s^{-1/2}\ r_s^{0.14}\ n_m^{-1/2}$ is also shown. Not only is the inferred resistivity higher (at least for low densities) on the LSX scaling, but simple $D_\perp \sim D_\perp(n)$ relationship does not appear to hold. A better result is obtained when $D_\perp$ is plotted versus the Bohm value, as shown in Fig. 4(b). It is to be noted that the diffusivity obtained in the previous translated FRTP produced hot FRCs is nearly a factor of ten lower than the data from present RMF formed FRCs but is consistent with the Bohm-like scaling trend. This suggests that the higher diffusivity obtained in the present RMF formed FRCs, compared to the conventional FRCs, may be resulted from low magnetic fields, or due to lack of hot ions. We are planning to apply the RMF current drive to the translated hot FRCs to investigate this.

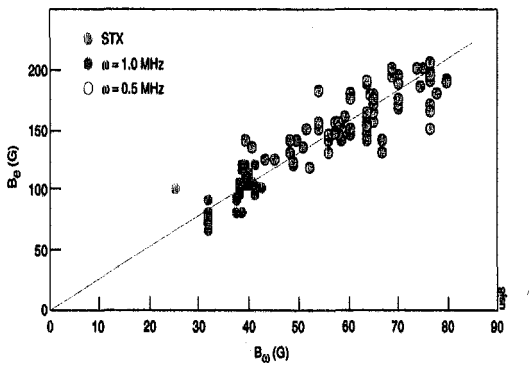

Figure 3. Be as a function of Bω for the cases: ω = 1.0 MHz and 0.5 MHz. STX data is also included

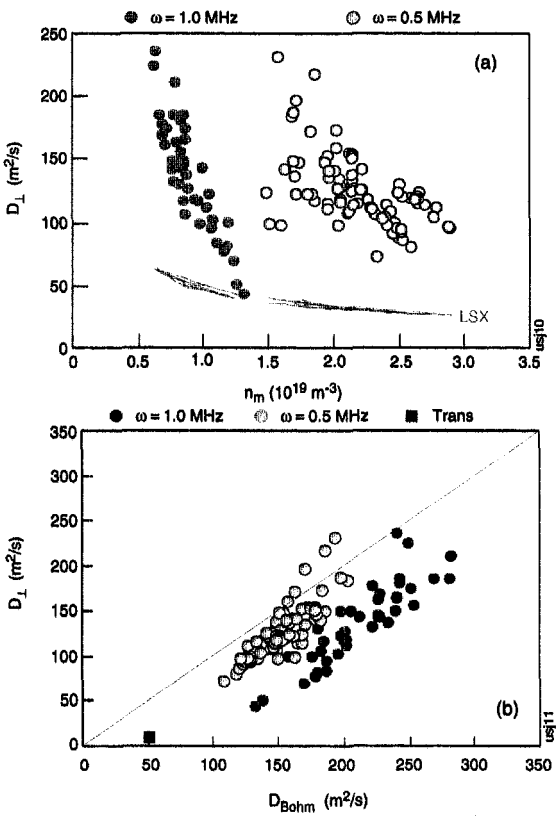

Figure 4. (a) $D_\perp$ versus nm; (b) $D_\perp$ versus D_{Bohm} scaling: D_{Bohm} = 625 Te(eV)/B(G) for the different cases.

3. Ion Spin-up

One critical issue with RMF current drive is that electrons rotating with the RMF lead to spin-up of ions in the RMF direction due to collisions with electrons, thus reducing the RMF current drive efficiency. It would take only ~100μs for ions to reach electron rotation speed with the present FRCs in TCS due to the high resistivity (nearly 20 times the classical value). This is, however, not

observed in the experiments. Ohnishi [2] showed in his analytical mode that ion rotation may be slowed down by transferring momentum with cold neutrals. The ion rotation speed is given as follows:

$$\alpha = \omega_i / \omega = 1 \Big/ \left(1 + \frac{m_i}{m_e} \frac{\upsilon_{in}}{\upsilon_\perp} \right) \qquad (3)$$

where υ_{in} is the momentum transfer frequency between ions and neutrals and $\upsilon_\perp$ the collision frequency between electrons and ions.

An ICCD camera is employed to routinely determine Doppler shifts of low charge state ions, viewing the plasma midplane on a number of lines of sight with different impact parameters. The multi-channel Doppler spectroscopy shows that C^{++} ions rotate in the same direction as RMF, presumably due to frictional drag by electrons.

To investigate spin-up process of ions, we have measured C^{++} rotation frequency at different times for a serious of repeatable discharges. The results are shown in Fig. 6 for the discharges performed with RMF frequency at ω = 1.0 MHz and 0.5 MHz, respectively. As shown in Fig. 6(a), it appears that the C^{++} speed is much higher in the reduced ω cases. This may have resulted from higher densities in the discharges with reduced RMF frequency, where mean-free path of neutrals before ionization is shorter, hence less neutrals are present in the plasma. To illustrate this, Fig. 6(b) shows the ratio of C^{++} ion speed to that of electrons as a function of electron density. Note the discharges with lower densities are correlated with lower ion rotation, consistent with the above analysis.

In addition, it is to be noted that the ions are spun up on a sub-hundred μs time scale, as expected. Variations in the speed during the discharges are possibly due to changes in plasma density, and thus neutral concentrations.

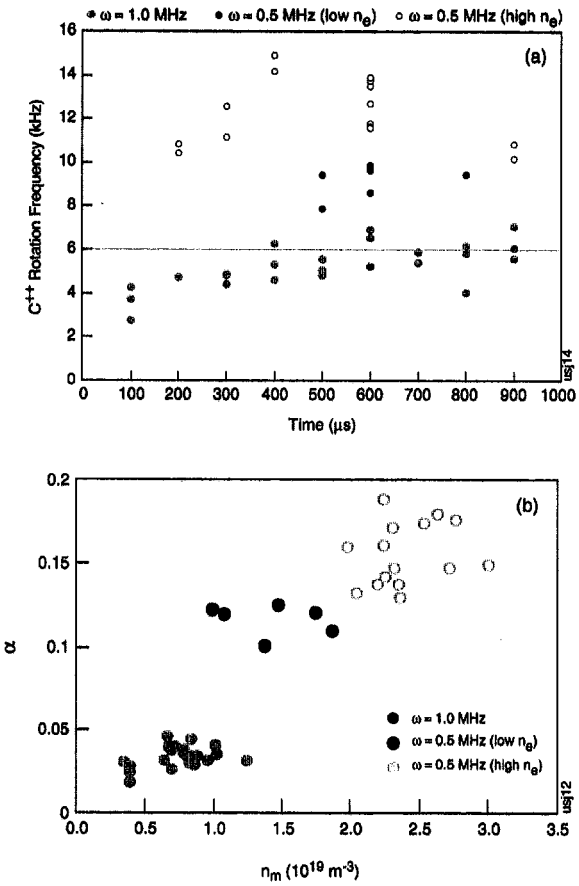

Figure 6. (a) C^{++} rotation frequency versus time; (b) Ratio of C^{++} spin up speed to electron rotation velocity versus electron density.

The number of neutrals required to slow down the ions can be estimated using Equation (3). For a typical discharge operated at the reduced ω: $n_e \sim 2\times10^{19}$ m^{-3}, $\eta_\perp \sim 150$ μΩ m, hence:

$$\nu_\perp = 28\eta_\perp(\mu\Omega m) n_e(10^{19} m^{-3}) \times 10^6 s^{-1}$$
$$= 8.4\times10^7 s^{-1}$$

From measured $\alpha = \omega_i / \omega \sim 0.15$, we can derive the required ion-neutral momentum transfer rate:

$$\nu_{in} = \left(1/\alpha - 1\right)\frac{m_e}{m_i}\gamma_\perp = 1.3\times10^5 s^{-1}.$$

With $T_i = T_e \sim 15eV$, charge exchange rate coefficient:

$$S_{cx} = \langle \sigma_{cx} v_i \rangle = 2.8\times10^{-14} m^3 s^{-1}.$$

Thus, the neutral concentration:

$$\frac{n_0}{n_e} = \frac{\nu_{in}}{n_e S_{cx}} = 23\%.$$

On the other hand, the neutral concentration can be estimated from global power balance. In steady state, RMF heating power is balanced by ionization, convection, charge exchange and radiation losses, neglecting conduction loss. In addition, the particle loss through convection channel should be balanced by the rate of ionization since recombination is negligible. Thus, we obtain:

$$P_{RMF} = n_e n_0 S_i V_0 \left[\varepsilon_i + \frac{5}{2}k(T_e + T_i)\right] + n_i n_0 S_{cx} V_0 \frac{3}{2}kT_i + P_{rad} \quad (4)$$

where P_{RMF} is heating power from RMF ($\int VIdt$ at antennae), S_i and S_{cx} are rate coefficients for ionization and charge change, respectively, V_0 is volume with neutrals presence, depending on mean free path of neutrals, ε_i is ionization energy (13.6eV per ionization), and P_{rad} is radiative power.

With $P_{RMF} \sim 2MW$, $P_{rad} \sim 0.5MW$, we obtain:

$$\frac{n_0}{n_e} \approx 16\%$$

which is consistent with estimation from ion rotation measurements.

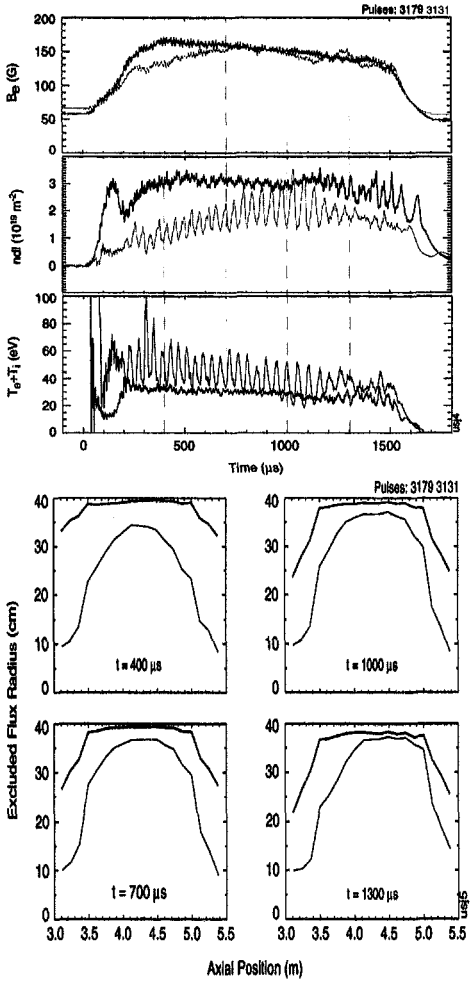

Figure 7. Evolution of two comparable discharges with different densities (upper) and Separatrix radius versus axial position for the two discharges at time slices marked in the top figure (lower).

4. Rotational Instability

Both n=1 off-center rotation mode and n = 2 mode have been observed in the RMF formed FRCs in TCS. The modes

tend to rotate in RMF direction. The observed rotational frequencies of the modes are in the range of tens of kHz, much slower than the RMF rotation speed.

The rotational modes are usually observed in low density discharges, as shown in Fig. 7(a) where plotted is the evolution of a lower density discharge, together with that of a typical steady state discharge case. In the lower density case, RMF field (B_ω, not shown) is also reduced due to changes in plasma inductance. However, similar external fields (B_e) are obtained, resulting from improved RMF penetration efficiency (higher ζ). Fig. 7(b) shows separatrix radius (r_s) as a function of axial position for the two discharges at the time slices marked in Fig. 7(a). It appears that the lower density FRC is shorter and further away from wall, facilitating growth of rotational modes.

In addition, r_s decreases with increasing bias field (B_0) due to flux conservation.

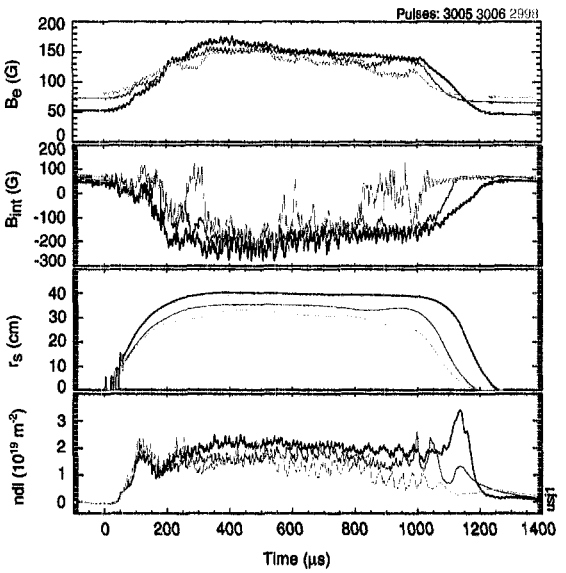

Figure 8. Evolution of three comparable discharges with different initial bias fields.

As a result, rotational modes tend to develop at high bias fields. Fig. 8 shows three comparable discharges with different bias fields. As can be seen, similar fields are obtained in pulses 3005 and 3006. However, in the highest bias case, the FRC is sufficiently further from the wall, and strong oscillations occurred, affecting field reversal.

5. Summary and Conclusions

- For the first time, steady state, flux confined FRCs are produced with $B_\omega << B_e$ using RMF current drive, and are well modeled by numerical calculations.
- Reducing ω to allow for more efficient penetration leads to improvements in RMF current drive, and production of higher density FRCs, as predicted by RMF current drive physics.
- In addition, at reduced ω, RMF antenna system delivers higher current (hence higher B_ω), thus allowing for more energetic FRCs.
- Ion spin-up in the RMF direction has been observed, but only up to ~20% RMF frequency most likely due to neutrals present in the machine. For hot FRCs, tangential neutral beam fuelling will probably be necessary to prevent ion spin-up.
- Rotational instabilities have been observed, but can be suppressed when FRC is sufficiently close to the wall, which is desired, anyway, for optimum RMF current drive.

[1] A.L. Hoffman, this workshop.

[2] M. Ohnishi, A. Ishida, Nucl. Fusion 36 (1996) 232.